Talanta 82 (2010) 1344–1348

Contents lists available at ScienceDirect

Talanta

journal homepage: www.elsevier.com/locate/talanta

Direct electrochemistry-based hydrogen peroxide biosensor formed from single-layer graphene nanoplatelet–enzyme composite film

Qing Lu, Xiaochen Dong, Lain-Jong Li, Xiao Hu*

School of Materials Science and Engineering, Nanyang Technological University, Singapore 639798, Singapore

ARTICLE INFO

Article history:
Received 22 April 2010
Received in revised form 28 June 2010
Accepted 28 June 2010
Available online 24 July 2010

Keywords:
Direct electrochemistry-based biosensor
Horseradish peroxidase
Single-layer graphene nanoplatelet
Tetrasodium 1,3,6,8-pyrenetetrasulfonic acid

ABSTRACT

A novel electrochemical sensing system for direct electrochemistry-based hydrogen peroxide biosensor was developed that relied on the virtues of excellent biocompatibility, conductivity and high sensitivity to the local perturbations of single-layer graphene nanoplatelet (SLGnP). To demonstrate the concept, the horseradish peroxidase (HRP) enzyme was selected as a model to form the SLGnP-TPA (tetrasodium 1,3,6,8-pyrenetetrasulfonic acid)–HRP composite film. The single-layer graphene composite film displayed a pair of well-defined and good reversible cyclic voltammetric peak for Fe(III)/Fe(II) redox couple of HRP, reflecting the enhancement for the direct electron transfer between the enzyme and the electrode surface. Analysis using electrochemical impedance spectroscopy (EIS) revealed that electrostatic attractions existed between graphene monolayers and enzyme molecules. The intimate graphene and enzyme interaction was also observed using scanning electron microscopy (SEM), which resulted in the special properties of the composite film. Ultraviolet visible spectroscopy (UV–vis) indicated the enzyme in the composite film retained its secondary structure similar to the native state. The composite film demonstrated excellent electrochemical responses for the electrocatalytic reduction of hydrogen peroxide (H_2O_2), thus suggesting its great potential applications in direct electrochemistry-based biosensors.

1. Introduction

Graphene and graphene-based materials have emerged to be fascinating materials from both perspectives of fundamental science and technology, because of their nontoxicity, chemical and thermal tolerance, electric conductivity and mechanical hardness [1,2]. These materials promise a wide-range of industrial applications, such as in energy storage, catalyst support, thermal transport media, structural and electronic components as well as in biotechnology [3–5]. Recently, single-layer graphene nanoplatelet (SLGnP) has attracted great attentions not only because its perfect two-dimensional carbon crystalline structure that enables unprecedented explorations of fundamental physics, but also because of its exciting potentials in the post-silicon nanoelectronics [6,7].

The rapid and accurate analysis of hydrogen peroxide (H_2O_2) is of great importance in many fields including food industry, clinical control and environmental protection. It is because that H_2O_2 is not only a by-product of several highly selective oxidases, but also an essential mediator in food, pharmaceutical, clinical, industrial and environmental analyses. Conventional techniques such as UV–vis spectrophotometry [8], chemiluminescence [9] and titrimetry [10] have been reported in literatures. However, the conventional methods are generally time-consuming and difficult for an automated detection. Besides, most of these methods show limitations such as lack of sensitivity and susceptibility to interference by other substances in analyte samples. To overcome all these shortcomings, the electrochemical biosensor based on the direct electrochemistry between an electrode and the immobilized enzyme/protein is especially promising because of its simplicity, high sensitivity and selectivity.

In a direct electrochemistry-based biosensor, biological molecules are integrated with electrodes, and the crucial step is the transfer of electrons to and from a biological molecule [11]. In many cases, however, there are several factors plagued the direct electrical communications between the redox center of enzymes/proteins and electrodes, including electroactive prosthetic groups deep within the protein structure, adsorptive denaturation of proteins onto electrodes and unfavorable orientations at electrodes [12]. According to Marcus theory [13], the electron transfer (ET) distance is a decisive factor for the direct electrochemistry of redox enzyme/protein, which depends on the overall distance between the redox site within the enzyme/protein and the electrode surface, and the orientation of the enzyme/protein on the electrode. As a consequence, for an optimally designed electrode configuration, the ET distance

* Corresponding author at: School of Materials Science and Engineering, Nanyang Technological University, Block N4.1, Nanyang Avenue, Singapore 639798, Singapore.
E-mail address: ASXHU@main.ntu.edu.sg (X. Hu).

0039-9140/$ – see front matter.
doi:10.1016/j.talanta.2010.06.061

should be short as possible. Nanomaterials are suitable for acting as "electronic wires" to shorten the ET distance and enhance the electron transfer between redox centers of the enzyme/protein and the electrode surface accordingly [14]. CNTs and CNTs-based composite materials are good examples [15,16].

Past studies have indicated that the electric properties of SLGnP film are extremely sensitive to local perturbations such as from surface charges and adsorbed gas molecules [17,18]. In addition, graphene sheets are essentially sp2 hybridized carbon atoms arranged in a two-dimensional structure. They are more affordable in comparison to the cylindrical CNTs, which have been widely studied [19,20]. SLGnP is biocompatible, high conductive and has large effective surface area. These characteristics are advantageous for their applications in direct electrochemistry-based biosensors.

In our previous work, it was found that the aromatic molecule, tetrasodium 1,3,6,8-pyrenetetrasulfonic acid (TPA), can effectively exfoliate graphite into SLGnP with good yield [21]. Thus, in this paper, by the simple method of mixing, an electrode with designed configuration was fabricated using the SLGnP–enzyme composite film. Here, horseradish peroxidase (HRP), a type of heme enzyme, was selected as a model for analysis. Direct electron transfer of the enzyme was achieved because SLGnP can provide a biocompatible microenvironment for enzyme immobilization and a suitable ET distance between electroactive center of the enzyme and the electrode surface. Moreover, the excellent electrocatalytic reduction ability for H_2O_2 showed the composite film can offer a feasible approach to the development of the direct electrochemistry-based biosensors.

2. Materials and methods

2.1. Chemicals

Horseradish peroxidase (HRP, MW 44,000) and tetrasodium 1,3,6,8-pyrenetetrasulfonic acid (TPA) were obtained from Sigma and used without further purification. Nafion (5 wt.% in lower aliphatic alcohols and water) was obtained from Sigma. In a typical experiment [21] for dispersing graphenes by TPA molecules, 1 mg graphite powders (NGS, Germany) was mixed with 10 mg TPA in 5 mL deionized (DI) water solution. And then, the mixture was sonicated by using a probe sonicator (pulse mode at 70 W) in an ice bath for 2 h. After gravity sedimentation over night and centrifugation the resulting supernatant was taken as SLGnP–TPA. All other chemicals were of analytical grade and used as obtained. All phosphate buffer solutions (PBS) were prepared using DI water from a Millipore Milli-Q water purification system. Enzyme solutions were stored at 4 °C prior to usage.

2.2. Preparation of the composite film

A glassy carbon (GC) electrode was first polished with 1.0, 0.3 and 0.05 μm alumina slurry, and then sonicated in nitric acid (1:1), ethanol and DI water in turn. HRP (1 mg/mL) in pH 5.0 PBS was mixed with SLGnP–TPA in 1:1 (V/V) ratio. Then, 5 μL of the mixture was applied to the freshly prepared GC electrode surface. The electrode was dried at ambient temperature over night. Finally, 1 μL Nafion (0.1%) was dropped onto the SLGnP–TPA–HRP film, which functions as a binder to hold the composite film on the electrode surface. The solvent was allowed to evaporate and the final electrode is taken as Nafion/SLGnP–TPA–HRP/GC electrode.

2.3. Apparatus

Cyclic voltammetry (CV) was performed by using a CHI660C electrochemical workstation (CH Instruments, Shanghai, China). A three-electrode system was employed, including a working

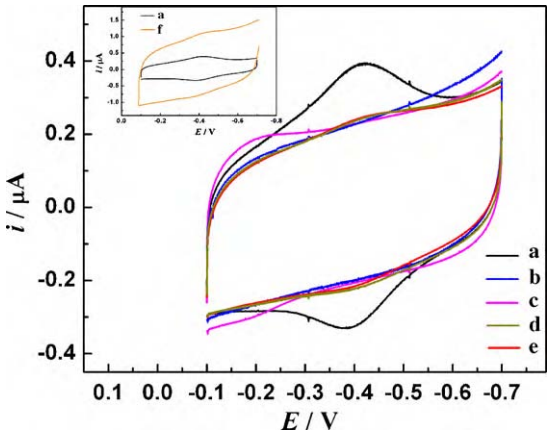

Fig. 1. Cyclic voltammograms at 0.1 V s^{-1} in pH 7.4 buffers for (a) Nafion/SLGnP–TPA–HRP film (dark), (b) the bare GC electrode (blue), (c) Nafion/SLGnP–TPA film (magenta), (d) Nafion/TPA–HRP film (dark yellow), (e) Nafion/HRP film (red), (f) Nafion/MLG–HRP film (orange). (For interpretation of the references to color in this figure legend, the reader is referred to the web version of the article.)

Nafion/SLGnP–TPA–HRP composite film electrode, a saturated calomel reference electrode (SCE) and a platinum wire counter electrode. Prior to each experiment, the buffer solutions were purged with high-purity nitrogen for at least 30 min and a nitrogen environment was then kept over the solution in the cell during experiments. All experiments were carried out at room temperature. Electrochemical impedance spectroscopy (EIS) was performed with an Autolab potentiostat/galvanostat (PGSTAT302, Echo Chemie B.V., The Netherlands) equipped with a frequency response analyzer module. All impedance data were recorded at an open circuit voltage with an amplitude of 10 mV over a frequency range of 0.1–100,000 Hz in 0.1 M KCl solution containing 10 mM $Fe(CN)_6^{3-}/Fe(CN)_6^{4-}$. Ultraviolet visible spectroscopy (UV–vis) was recorded with a Shimadzu UV2501 spectrophotometer (Japan).

3. Results and discussion

3.1. Electrochemical characteristics of SLGnP–TPA–HRP composite film

The electrochemical behavior of SLGnP–TPA–HRP composite film was analyzed by CV, using Nafion as a binder. To discern the role of individual components, films of Nafion/TPA–HRP, Nafion/HRP, Nafion/SLGnP–TPA and the bare GC electrode were also studied in 0.1 M PBS (pH 7.4). The utilization of SLGnP as an immobilizing compound for enzyme can provide a useful sensing system and offer great promise for direct electron transfer of enzyme. This electrochemical sensing behavior is illustrated in Fig. 1, showing that the Nafion/SLGnP–TPA–HRP film modified GC electrode yields a pair of well-defined and quasi-reversible redox peaks (curve a). However, no redox peaks appear at the bare GC electrode (curve b) and Nafion/SLGnP–TPA film modified GC electrode (curve c). Curves d and e in Fig. 1 also show the relatively featureless cyclic voltammograms of Nafion/TPA–HRP and Nafion/HRP films, respectively. This suggests that the electrochemical reaction of HRP at a bare electrode and TPA film modified electrode have little contributions to the observed redox peaks in curve a. These results clearly illustrate that the pair of peaks in curve a is the characteristic of Fe(III)/Fe(II) redox couple for HRP, and SLGnP plays the primary and essential role for the enhancement of protein's direct electron transfer. The anodic peak potential (E_{pa}) and the cathodic peak potential (E_{pc}) are located at about −0.387 V and −0.425 V, respectively, and the ratio of the cathodic

current of the anodic one is about 1. The formal potential ($E^{o\prime}$), defined as the average of E_{pa} and E_{pc}, is about −0.406 V, similar to that of HRP immobilized on CNTs [22]. The separation of the peak potential (ΔE_p) is 38 mV, in excess of the ideal thin-film value of 0 mV [23]. All these values coincide well with the behavior of the direct electrochemistry of heme Fe(III)/Fe(II) couples of the proteins [24,25]. In addition, the ΔE_p value of SLGnP–TPA–HRP film is much smaller than that of HRP–CNTs reported in the literature [22], indicating the better direct electron transfer enhancement of SLGnP, which ascribes to the unique characteristics of graphene. For further comparison, multiple layered graphene (MLG) was used to immobilize HRP at the GC electrode, instead of SLGnP–TPA. The Nafion/MLG–HRP film modified GC electrode gives a pair of unconspicuous redox peaks (Fig. 1, curve f) with a peak-to-peak separation of about 65 mV. This value is much larger than that of SLGnP–TPA–HRP film, suggesting the unique electrochemical properties of SLGnP for the direct electrochemistry of HRP.

The effect of the scan rate on the electrochemical response of SLGnP–TPA–HRP film was also investigated by CV. The results displayed that the reduction and oxidation peak currents of the composite film exhibited a linear relationship with the scan rate from 0.04 to 0.5 V s^{-1} (r = 0.996). And the charge (Q) consumed in coulombs, obtained from integrating the anodic or cathodic peak area in CVs, was nearly constant and independent of scan rates in the same range. In addition, both the $\log i_{pc} - \log \nu$ and $\log i_{pa} - \log \nu$ plots illustrated linear relationship, with the ratio of the slopes about one. All these results suggested that the electrochemical reaction of SLGnP–TPA–HRP film was a surface-confined or thin-layer electrochemical behavior [26]. During this process, all electroactive ferrous enzymes (enzyme–Fe(II)), which were produced by the reduction of ferric enzymes (enzyme–Fe(III)) on the cathodic scan, could be oxidized to enzyme–Fe(III) on the anodic scan. The surface concentration of electroactive HRP (Γ^*) could be calculated according to the Faraday's law:

$$Q = nFA\Gamma$$

where Q is the charge involved in the reaction, n is the number of transferred electron, F is the Faraday's constant, and A is the effective area of the GC electrode. Because the Q values were nearly constant in the range of scan rates from 0.04 to 0.5 V s^{-1}, the surface concentration of electroactive HRP (Γ^*) for SLGnP–TPA–HRP film was constant with an average value of 5.68×10^{-11} mol/cm^2. Compared with the total amount of HRP modified on the electrode (estimated to be 3.25×10^{-10} mol/cm^2), there was about 17.5% of total amount of HRP deposited on the electrode involved in the electron-transfer reaction. The apparent heterogeneous electron transfer rate constant k_s of HRP in SLGnP–TPA film could be estimated by using the equation derived by Laviron for diffusionless CV [27]. The average value of k_s was 3.5 s^{-1}, suggesting reasonably fast electron transfer. For MLG–HRP film, k_s was estimated to be 2.1 s^{-1}, lower than that of SLGnP–TPA–HRP film. It also confirmed the better enhancement of SLGnP for the direct electron transfer of HRP.

The external solution pH can modulate the accessibility of water to the heme pocket of HRP and the protonation of the heme iron-bound proximal histidine and/or the distal histidine in the heme pocket. Consequently, the redox potential of SLGnP–TPA–HRP film showed a strong dependence on the external solution pH. With the increase of the solution pH value, both E_{pa} and E_{pc} shifted to a negative direction, while the redox peak shapes kept nearly unchanged. This phenomenon indicated a proton transfer involved redox reaction. In general, all changes in CV peaks with the change of pH were reversible between pH 3.0 and 9.0. Within the above pH range, E_{pa}, E_{pc} and $E^{o\prime}$ were dependent on the solution pH linearly with the slopes of −42 mV/pH, −40 mV/pH and −41 mV/pH, respectively. Those slope values were much smaller than the theoretical value of −59 mV/pH for a single-proton coupled, reversible one-electron transfer [28]. Processes involving coupled electron and proton transfer are often tuned by the electrostatic interaction between the metal center and the charged sites in the vicinity of the heme group [29,30]. With the shift of external solution pH, the protonation state of *trans* ligands to the heme iron varies, resulting in the change of charges possessed by the metal center. On the other hand, the external solution pH also influences the protonation of amino acids around the heme and the water molecules coordinated to the central iron, leading to the variation of charges around the heme group. Combined the two actions above, the shift in $E^{o\prime}$ as a function of pH does not simply follow the ideal law for a single-proton coupled, reversible one-electron transfer. Thus, the slopes of the plots of E versus pH were much smaller than the theoretical value.

3.2. Characteristics of SLGnP–TPA–HRP composite film

Scanning electron microscopy (SEM) was used to characterize and compare the surface morphologies of HRP, SLGnP–TPA and SLGnP–TPA–HRP films on a GC block, as shown in Fig. 2. The HRP film displays a rough and apertured structure (Fig. 2A). In view of abundant sulfonic groups of TPA, SLGnP dispersed by TPA molecules has negative charges. Thus, its SEM image gives foliiform patched morphology (Fig. 2B) due to the charge repulsion. On the other hand, the isoelectric point of HRP is 7.2. So the enzyme dissolved in pH 5.0 PBS has positive charges. When the enzyme and SLGnP–TPA are mixed together, there are electrostatic attractions between them due to the different charges they have. The electrostatic attractions also reduced the charge repulsion between TPA molecules. Accordingly, the SEM image of the composite film demonstrates a smooth and homogeneous mixed configuration, with a few pieces of SLGnP–TPA patches exposed (Fig. 2C). The difference of the morphologies reflects that strong interactions take place between HRP and SLGnP–TPA, which have influence on the structure of the composite film. The results also support our earlier hypothesis that the unique sheet-like structure of graphene is likely to result in intimate interaction with both electrode materials and enzymes/proteins, making it a superior candidate for biosensor applications.

Electrochemical impedance spectroscopy (EIS) was performed in order to investigate the interactions between HRP and

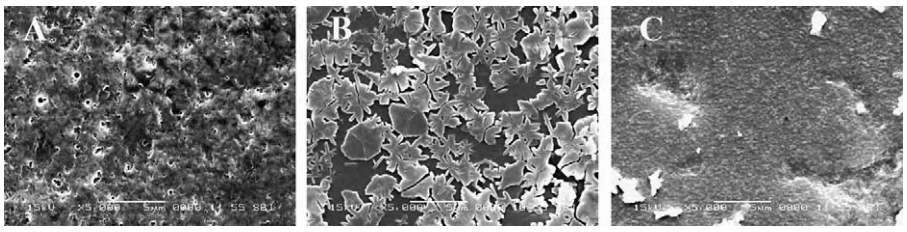

Fig. 2. SEM images with the same magnification of (A) HRP film, (B) SLGnP–TPA film and (c) SLGnP–TPA–HRP composite film at a GC block.

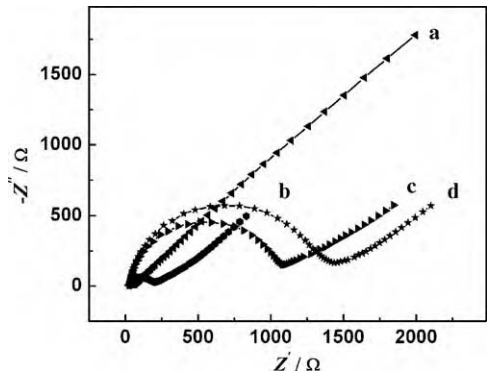

Fig. 3. Impedance plane diagram ($-Z''$ versus Z') for the EIS measurements on (a) the bare GC electrode, (b) Nafion/SLGnP–TPA/GC electrode, (c) Nafion/HRP/GC electrode, (d) Nafion/SLGnP–TPA–HRP/GC electrode in 0.1 M KCl solution containing 10 mM $Fe(CN)_6^{3-}$/$Fe(CN)_6^{4-}$ (1:1).

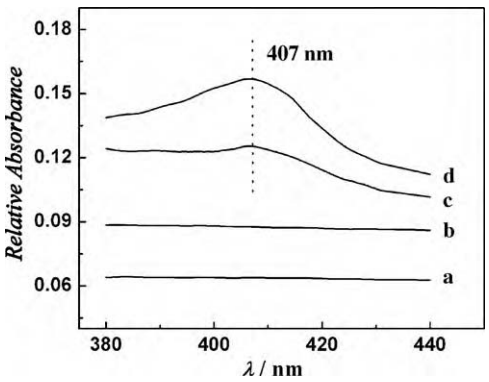

Fig. 4. UV–vis spectra of dry (a) SLGnP–TPA film, (b) TPA film, (c) SLGnP–TPA–HRP film and (d) HRP film. The absorbance coordinate only reflects relative absorbance.

SLGnP–TPA further. Fig. 3 displays the EIS profiles of different films, in which the Nyquist plots are shown with the real part (Z') on the X-axis and the imaginary part ($-Z''$) on the Y-axis. For the diffusive species (referring to ferricyanide), the spectrum includes a semicircle part and a linear part, of which the semicircle part at high frequencies corresponds to the electron transfer limited process and the linear part at low frequencies corresponds to the diffusion process. And the diameter of the semicircle portion corresponding to the electron transfer limited process equals to the electron-transfer resistance (R_{ct}). The lowest R_{ct} on the bare GC electrode (curve a) indicates the fastest electron transfer rate between the bare electrode and ferricyanide. Because SLGnP has excellent conductivity, the R_{ct} of the electrode modified with SLGnP–TPA film only increases a little (curve b). However, the R_{ct} of the HRP film modified electrode increases dramatically, owing to the insulation of enzyme (curve c). The insulation of HRP also results in the increasing R_{ct} for the SLGnP–TPA–HRP film (curve d). In addition, the R_{ct} value for the SLGnP–TPA–HRP film is a little larger than that of the HRP film, which ascribes to the electrostatic interactions between HRP and SLGnP–TPA. The enzyme dissolved in pH 5.0 PBS has positive charges, which will adsorb ferricyanide. While SLGnP–TPA has negative charges that will block $Fe(CN)_6^{3-}$ and $Fe(CN)_6^{4-}$. When they are mixed together, there are electrostatic attractions between them due to the different charges they have. Thus, the neutralization of charges will reduce the effect of adsorption for $Fe(CN)_6^{3-}$ and $Fe(CN)_6^{4-}$ and increase the R_{ct} value as a result.

The Soret absorption band of heme protein is sensitive to its microenvironment, substructure, and oxidation state [26]. Thus, in general, ultraviolet visible spectroscopy (UV–vis) is always used to verify whether the heme protein molecules have denatured or not. Fig. 4 exhibits the UV–vis spectra of dry TPA, HRP, SLGnP–TPA and SLGnP–TPA–HRP films. As expected, there are no UV–vis absorptions for TPA (curve b) and SLGnP–TPA (curve a) films. And the Soret band of HRP in SLGnP–TPA film is located at 407 nm (curve c), which is virtually identical to that of a native HRP film (curve d). The UV–vis results indicate the enzyme can maintain its natural structure in the composite film, which is particularly critical in order to keep the enzyme functional in its incorporated film.

3.3. Electrocatalytic properties of SLGnP–TPA–HRP composite film

The enzyme, HRP, has long been a representative system for investigating the structure, dynamic and thermodynamic properties of peroxidase family, and especially for elucidating their biological behaviors to catalyze oxidation of substrates by hydrogen peroxide (H_2O_2). Since SLGnP has the virtue of excellent biocompatibility, the composite film can maintain the electrocatalytic properties of the enzyme. In particular, the composite film showed sensitive and fast catalytic activity towards H_2O_2, owing to SLGnP's electrical sensitivity to the local perturbations.

The electrocatalytic properties of the SLGnP–TPA–HRP composite film were tested by CV. And a typical catalytic reduction peak of H_2O_2 at Nafion/SLGnP–TPA–HRP film is shown in Fig. 5A. Comparing with the Nafion/SLGnP–TPA–HRP film in the absence of H_2O_2 (curve c), when H_2O_2 (2.1×10^{-6} M) is added into the electrochemical cell, an increase of the reduction peak at about −0.38 V is observed and accompanied by the decrease of the oxidation peak (curve d), suggesting a typical electrocatalytic reduction process of H_2O_2. However, no difference in the CV curves is seen whether in the absence (curve a) or in the presence (curve b) of H_2O_2 for Nafion/SLGnP–TPA film. This means that only the enzyme can catalyze the reduction of H_2O_2. In addition, the H_2O_2 reduction peak current increases with the addition of H_2O_2 (6.3×10^{-6} M) in buffer (curve e). The plot (Fig. 5B, inset) shows that the H_2O_2 reduction peak current has a linear relationship with its concentration in the range of 6.3×10^{-7} to 1.68×10^{-5} M in the buffer solution. And the linear regression equation is I (μA) = 0.171 + 0.0212 (C/μM), with a correlation coefficient 0.996 (n = 11). The detection limit was 1.05×10^{-7} M at a signal-to-noise ratio of 3, a very low value compared with other systems (such as 9×10^{-6} M for HRP–clay–chitosan–gold nanoparticle nanocomposite and 1.7×10^{-6} M for HRP–toluidine blue–multiwalled carbon nanotubes nanocomposite) [14,16]. When the concentration of H_2O_2 in buffer is higher than 2.3×10^{-5} M, the calibration curve runs to a plateau and then falls down with continuous addition of H_2O_2 (Fig. 5B), indicating a progressive enzyme inactivation at the presence of higher concentration of H_2O_2 that can be explained with a Michaelis–Menten kinetics model. As a reflection of both the enzymatic affinity and the ratio of microscopic kinetic constants, K_m^{app}, the apparent Michaelis–Menten constant, can be calculated from the electrochemical version of the Lineweaver–Burk equation [31]:

$$\frac{1}{I_{ss}} = \frac{1}{I_{max}} + \frac{K_m^{app}}{I_{max}C}$$

where I_{ss} is the steady-state current after the addition of substrate, I_{max} is the maximum current measured under saturated substrate conditions and C is the bulk concentration of the substrate. Here, the value of K_m^{app} for SLGnP–TPA–HRP is estimated to be 11.02 μM. This value is much smaller than that of 1350 μM for HRP–SG–CNT film [32], suggesting that the present composite film exhibits a higher affinity for H_2O_2.

The composite film also revealed good amperometric responses for the electrocatalytic reduction of H_2O_2. With the addition of

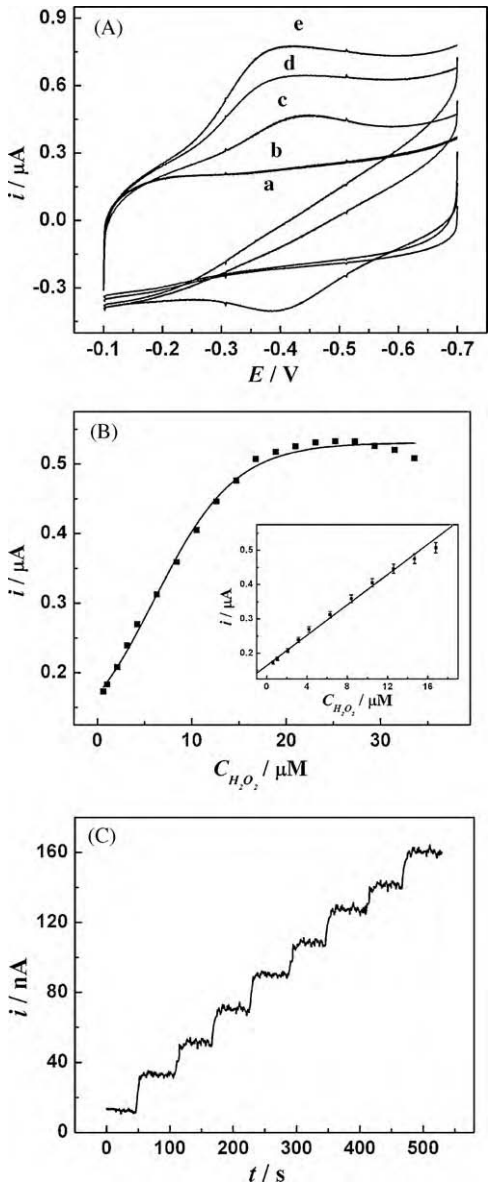

Fig. 5. (A) Cyclic voltammograms at 0.1 V s^{-1} in pH 7.4 buffer for (a) SLGnP–TPA and (c) SLGnP–TPA–HRP films without H_2O_2, (b) SLGnP–TPA and (d) SLGnP–TPA–HRP films in buffer containing 2.1 μM H_2O_2, (e) SLGnP–TPA–HRP film in buffer containing 6.3 μM H_2O_2. (B) Calibration curve of the reduction peak currents against the concentration of H_2O_2. The inset is the linear relative plot. (C) Amperometric responses at Nafion/SLGnP–TPA–HRP/GCE at the potential of −0.45 V in 5 mL PB buffer (pH 7.4) with injecting 0.42 μM H_2O_2 every 30 s.

an aliquot of H_2O_2 to the buffer solution, the reduction current increases rapidly to reach a stable value. The SLGnP–TPA–HRP film modified GC electrode reaches 95% of the steady-state current in <1 s, showing a very fast electrocatalytic response. Upon successive additions of 0.42 μM H_2O_2 to the electrochemical cell, a good amperometric curve is obtained (Fig. 5C).

The SLGnP–TPA–HRP film modified GC electrode showed a good stability. When the composite film modified electrode was stored at 4 °C in refrigerator for about 10 days, it still retained about 92% of its initial sensitivity to the reduction of H_2O_2. And the reproducibility of the Nafion/SLGnP–TPA–HRP/GC electrode was estimated at a buffer solution containing H_2O_2 concentration of 2.1 μM with the same modified electrode. The relative standard deviation (RSD) was 4.48% (n = 8). Ascorbic acid, one of the main interferences in a biological fluid, was investigated for the detection of H_2O_2 with the Nafion/SLGnP–TPA–HRP/GC electrode by amperometry. Only insignificantly additional amperometric signal appeared in pH 7.4 buffer containing 10.5 μM H_2O_2 with addition of ascorbic acid more concentrated than H_2O_2 by 20 times.

4. Conclusions

In summary, a new type of direct electrochemistry-based hydrogen peroxide biosensor was created with the utilization of the single-layer graphene nanoplatelet–enzyme composite film. Since SLGnP has the virtues of excellent biocompatibility, super conductivity and high sensitivity to the local perturbations, the composite film cannot only enhance the direct electron transfer between the enzyme and the electrode surface, but also offer the third-generation biosensor with good properties, such as fast response and high sensitivity. This system also adapts to other enzymes, such as glucose oxidase, catalase and xanthine oxidase. It will provide a new aspect for the fabrication of mediator-free biosensors.

Acknowledgment

This work is financially supported under a program funded by National Research Foundation of Singapore (NRF-G-CRP-2007-01).

References

[1] K.S. Novoselov, A.K. Geim, S.V. Morozov, D. Jiang, Y. Zhang, S.V. Dubonos, I.V. Grigorieva, A.A. Firsov, Science 306 (2004) 666–669.
[2] L.A. Ponomarenko, F. Schedin, M.I. Katsnelson, R. Yang, E.W. Hill, K.S. Novoselov, A.K. Geim, Science 320 (2008) 356–358.
[3] A.K. Geim, K.S. Novoselov, Nat. Mater. 6 (2007) 183–191.
[4] K.S. Novoselov, Z. Jiang, Y. Zhang, S.V. Morozov, H.L. Stormer, U. Zeitler, J.C. Maan, G.S. Boebinger, P. Kim, A.K. Geim, Science 315 (2007) 1379.
[5] S. Watcharotone, D.A. Dikin, S. Stankovich, R. Piner, I. Jung, G.H.B. Dommett, G. Evmenenko, S.E. Wu, S.F. Chen, C.P. Liu, S.T. Nguyen, R.S. Ruoff, Nano Lett. 7 (2007) 1888–1892.
[6] Y. Zhang, Y.W. Tan, H.L. Stormer, P. Kim, Nature 438 (2005) 201–204.
[7] M.Y. Han, B. Ozyilmaz, Y. Zhang, P. Kim, Phys. Rev. Lett. 98 (2007) 206805–206809.
[8] C. Matsubara, N. Kawamoto, K. Takamala, Analyst 117 (1992) 1781–1784.
[9] K. Nakashima, K. Maki, S. Kawaguchi, S. Akiyama, Y. Tsukamoto, K. Imai, Anal. Sci. 7 (1991) 709–714.
[10] A.I. Vogel, Textbook of Quantitative Chemical Analysis, Longman, U.K., 1989.
[11] I. Willner, E. Katz, Angew. Chem. Int. Ed. 39 (2000) 1181–1218.
[12] J.F. Rusling, Acc. Chem. Res. 31 (1998) 363–369.
[13] R.A. Marcus, Angew. Chem. Int. Ed. Engl. 32 (1993) 1111–1121.
[14] X. Zhao, Z. Mai, X. Kang, X. Zou, Biosens. Bioelectron. 23 (2008) 1032–1038.
[15] C.X. Cai, J. Chen, Anal. Biochem. 325 (2004) 285–292.
[16] Y. Liu, J. Lei, H. Ju, Talanta 74 (2008) 965–970.
[17] J. Martin, N. Akerman, G. Ulbricht, T. Lohmann, J.H. Smet, K.V. Klitzing, A. Yacoby, Nat. Phys. 4 (2008) 144–148.
[18] F. Schedin, A.K. Geim, S.V. Morozov, E.W. Hill, P. Blake, M.I. Katsnelson, K.S. Novoselov, Nat. Mater. 6 (2007) 652–655.
[19] J. Lu, L.T. Drzal, R.M. Worden, I. Lee, Chem. Mater. 19 (2007) 6240–6246.
[20] J. Lu, I. Do, L.T. Drzal, R.M. Worden, I. Lee, ACS Nano 2 (2008) 1825–1832.
[21] X.C. Dong, Y.M. Shi, Y. Zhao, D.M. Chen, J. Ye, Y.G. Yao, F. Gao, Z.H. Ni, T. Yu, Z.X. Shen, Y.X. Huang, P. Chen, L.J. Li, Phys. Rev. Lett. 102 (2009) 135501.
[22] H.J. Jiang, C. Du, Z.Q. Zou, X.W. Li, D.L. Akins, H. Yang, J. Solid State Electrochem. 13 (2009) 791–798.
[23] R.W. Murray, in: A.J. Bard (Ed.), Electroanalytical Chemistry, Marcel Dekker, New York, 1984.
[24] A.C. Onuoha, J.F. Rusling, Lagmuir 11 (1995) 3296–3301.
[25] S.M. Chen, C.C. Tseng, J. Electroanal. Chem. 575 (2005) 147–160.
[26] J.F. Rusling, A.E.F. Nassar, J. Am. Chem. Soc. 115 (1993) 11891–11897.
[27] E. Laviron, J. Electroanal. Chem. 101 (1979) 19–28.
[28] A.M. Bond, Modern Polarographic Methods in Analytical Chemistry, Marcel Dekker, New York, 1980.
[29] I. Yamazaki, T. Araiso, Y. Hayashi, H. Yamada, R. Makino, Adv. Biophys. 11 (1978) 249–281.
[30] H.H. Liu, Z.Q. Tian, Z.X. Lu, Z.L. Zhang, M. Zhang, D.W. Pang, Biosens. Bioelectron. 20 (2004) 294–304.
[31] R.A. Kamin, G.S. Willson, Anal. Chem. 52 (1980) 1198–1205.
[32] J. Wang, M. Gu, J. Di, Y. Gao, Y. Wu, Y. Tu, Bioprocess Biosyst. Eng. 30 (2007) 289–296.